J. Phys. B: Atom. Molec. Phys., Vol. 8, No. 7, 1975. Printed in Great Britain.

Electron impact excitation of H and He^+ III. 1s → *n*p transitions

M R C McDowell†, L A Morgan‡ and Valerie P Myerscough§

† Mathematics Department, Royal Holloway College, Englefield Green, Surrey, England
‡ Department of Computer Science, Royal Holloway College, Englefield Green, Surrey, England
§ Applied Mathematics Department, Queen Mary College, London, England

Received 6 September 1974, in final form 21 November 1974

Abstract. The distorted wave polarized orbital models described in papers I and II are used to calculate total and differential cross sections for 1s → *n*p ($n = 2, 3, 4$) transitions in H and He^+. The calculated total 2p cross sections agree with experiment within ±10% at all energies above 20 eV. Differential cross sections for total $n = 2$ excitation are in good agreement with experiment at 50 eV and angles below 60°. The predictions for 90° polarization of Ly α also agree closely with experiment for $E \geqslant 20$ eV.

1. Introduction

In this paper we extend our distorted wave polarized orbital calculations (McDowell *et al* 1973, 1974, to be referred to as I and II respectively), for electron impact excitation of H and He^+ to 1s → *n*p transitions ($n = 2, 3, 4$). A preliminary calculation on the 1s → 2p transition in atomic hydrogen has been reported by Lloyd and McDowell (1969) at a few energies, but they restricted themselves to total cross sections.

Our model is a single-channel one and does not attempt to deal with resonance structure near inelastic thresholds; but we expect it to be useful at energies above the ionization threshold and below the region of validity of the first Born approximation. At high energies our results tend to the CBO I approximation of Burgess *et al* (1970) for $Z \neq 1$, and to the Born and Born–Oppenheimer approximations for $Z = 1$. However in addition we take into account distortions due to the short-range static local potential of the target ground state, and to the long-range Callaway–Temkin polarization potential.

For the 1s → 2p transition we also consider off-diagonal s–p coupling via polarization of the target, as in II, and we refer to this improved model as the DWPO II.

It would be inappropriate to attempt to review all other relevant theoretical treatments of the transitions studied. Important recent calculations for the transitions of interest include the Coulomb-projected Born approximation (Geltman and Hidalgo 1971), the Glauber approximation (Gerjuoy and Thomas 1974 and reference therein), the eikonal–Born series method (Byron and Joachain 1973 and references therein), the many-channel eikonal method (Flannery and McCann 1974) and the second-order optical potential method of Bransden *et al* (1972). A more detailed comparison of the available methods for the theoretical study of electron impact excitation of H and He will be given elsewhere (McDowell 1975).

In this paper the emphasis will be on results for total cross sections, polarization of Ly α, and low energy differential cross sections.

Differential cross sections for excitation of the 2s and 2p states at energies above 50 eV will be presented in a separate paper (V).

A further paper (IV) will present our analysis and prediction of results for possible Ly α–electron coincidence experiments.

Experimental measurements of total cross sections for $e+H(1s) \rightarrow e+H(2p)$ are available (Long *et al* 1968, McGowan *et al* 1969, Williams and Willis 1974) and some new measurements for the $n = 3$ total cross section are in progress (Mahan *et al* 1975, see also Mahan 1974), to complement the earlier work (Kleinpoppen and Kraiss 1968, McGowan *et al* 1969). These new measurements also provide values for the 3s, 3p and 3d cross sections separately.

The polarization of the Ly α radiation emitted at 90° to the incident electron beam has been measured by Ott *et al* (1970) and provides a further check on our calculations. Recent absolute measurements of the differential cross section for the 2p transition (Bohm 1974, Williams and Willis 1975) will also be discussed.

We summarize our formulae for the observable parameters in § 2 (the theoretical formulation having been given in I), and outline our numerical methods in § 3. Our results are presented and compared with experiment in § 4. Finally we present our conclusions in § 5.

2. Theory

We adopt the notation of I. In the model of that paper (§ 2), superscripts referring to singlet (+) and triplet (−) states, the T-matrix elements for the $1s \rightarrow np\mu$ transition are

$$T^{\pm}_{1s\rightarrow np\mu} = \langle \phi_{np\mu}(Z, 1)\chi_{\boldsymbol{k}_f}(\mathscr{Z}, 2)|V_f|(1 \pm P_{12})\phi_{1s}(1)F^{\pm}(2)\rangle. \tag{1}$$

After carrying out the angular integrations we have for $\mu = 0$,

$$T^{\pm}_{1s\rightarrow np0} = \sum_{l=0}^{\infty} C_l^{\pm} P_l(\cos\theta) \tag{2}$$

where (except for $l = 0$, cf (9) below),

$$C_l^{\pm} = \frac{4\pi}{\sqrt{k_i}} \frac{i}{\sqrt{3}} [(l+1)\exp(i\zeta^{\pm}_{l,l+1})K^{\pm}(l, l+1) - l\exp(i\zeta^{\pm}_{l,l-1})K^{\pm}(l, l-1)]. \tag{3}$$

The phase parameters ζ are given by

$$\zeta^{\pm}_{l,l\pm1} = \delta^{\pm}_{l\pm1}(k_i) + \eta_{l\pm1}(k_i) - \eta_l(k_f), \tag{4}$$

and the matrix elements K may be written as

$$K^{\pm}(l, l\pm1) = I^{\pm}(l, l\pm1) \pm \frac{3}{(2l+1)} J^{\pm}(l, l\pm1). \tag{5}$$

The basic integrals are

$$I^{\pm}(l, l\pm1) = \int_0^{\infty} U^{(\pm)}_{l\pm1}(k_i, r) H_l(k_f, r) r f_{1s,np}(r)\, dr \tag{6}$$

with

$$f_{1s,np}(r) = \int_0^\infty R_{1s}(t)R_{np}(t)\gamma_1(r, t)t^2 \, dt, \tag{7}$$

and

$$J^{\pm}(l, l\pm 1) = \int_0^\infty U^{(\pm)}_{l\pm 1}(k_1, r)R_{np}(r)g_{1s,l}(r) \, dr \tag{8}$$

where $g_{1s,l}$ is defined in (I.32). However $l = 0$ is a special case with

$$C_0^{\pm} = \frac{4\pi}{\sqrt{3k_i}} i \exp(i\zeta^{\pm}_{0,1})\left(K^{\pm}(0, 1) \mp \frac{6Z^{3/2}d(\alpha_f)}{Z^2 + k_f^2}\int_0^\infty R_{np}(r)U_1^{\pm}(k_i, r)r \, dr\right) \tag{9}$$

and

$$d(\alpha_f) = \left(\frac{2\pi\alpha_f}{e^{2\pi\alpha_f} - 1}\right)^{1/2} \exp[2\alpha_f \tan^{-1}(k_f/Z)] \tag{10}$$

is a Coulomb screening factor in which

$$\alpha_f = -\mathscr{Z}/k_f, \qquad \mathscr{Z} = Z - 1 \qquad \text{and} \qquad d(0) = 1.$$

A similar analysis may be carried through for $\mu = \pm 1$ to yield

$$T^{\pm}_{if,\mu} = \sum_{l=1}^{\infty} F_l^{\pm} P_l^1(\cos\theta) \tag{11}$$

with

$$F_l^{\pm} = \frac{4\pi}{\sqrt{k_i}} \frac{i^{\mu}}{\sqrt{6}}[\exp(i\zeta^{\pm}_{l,l+1})K^{\pm}(l, l+1) + \exp(i\zeta^{\pm}_{l,l-1})K^{\pm}(l, l-1)]. \tag{12}$$

The total cross sections for the processes $1s \rightarrow np\mu$ ($\mu = 0, \pm 1$) become

$$Q_{1s\rightarrow 2p0}(k_i^2) = \frac{1}{4\pi^2}\frac{k_f}{k_i}\sum_{l=0}^{\infty}\frac{1}{(2l+1)}[|C_l^+|^2 + 3|C_l^-|^2] \tag{13}$$

and

$$Q_{1s\rightarrow 2p\pm 1}(k_i^2) = \frac{1}{4\pi^2}\frac{k_f}{k_i}\sum_{l=1}^{\infty}\frac{l(l+1)}{2l+1}[|F_l^+|^2 + 3|F_l^-|^2]. \tag{14}$$

Summing over final states and averaging over the (single) initial state gives

$$Q_{1s\rightarrow np}(k_i^2) = \frac{1}{4\pi^2}\frac{k_f}{k_i}\sum_{l=0}^{\infty}\frac{1}{(2l+1)}[|X_l^+|^2 + 3|X_l^-|^2], \tag{15}$$

the $|X_l^{\pm}|^2$ being given by the simple expressions

$$|X_l^{\pm}|^2 = \frac{(4\pi)^2}{3k_i}(2l+1)[(l+1)K^{\pm}(l, l+1)^2 + lK^{\pm}(l, l-1)^2] \tag{16}$$

for $l \geqslant 1$, and for $l = 0$

$$|X_0^{\pm}|^2 = \frac{(4\pi)^2}{3k_i}\left(K^{\pm}(0, 1) \mp \frac{6Z^{3/2}d(\alpha_f)}{(Z^2 + k_f^2)}\int_0^\infty R_{np}(r)U_1^{\pm}(k_i, r)r \, dr\right)^2.$$

We note here that (as in I) by omitting the local static potential $V_{1s,1s}(r)$ and the Callaway–Temkin polarization potential, $V_{pol}(r)$, together with the zero-order exchange term from the integro-differential equation (I.11) whose solutions are the distorted waves, $U_l^{\pm}(k_i, r)$ our model reduces to the CBO I approximation of Burgess *et al* (1970). In making direct comparison it should be noted that our partial wave sums refer to the scattered electron, while Burgess *et al* sum over those of the incident electron.

2.1. Differential cross sections

We have for the partial differential cross section corresponding to excitation of the $2p\mu$ state,

$$\sigma_\mu(\theta) = \frac{1}{4\pi^2}\frac{k_f}{k_i}[\tfrac{1}{4}|T_{if}^+|^2 + \tfrac{3}{4}|T_{if}^-|^2]\, a_0^2 \mathrm{sr}^{-1}. \tag{17}$$

Making a partial wave expansion and considering first $\mu = 0$,

$$\sigma_0(\theta) = \frac{1}{16\pi^2}\frac{k_f}{k_i}\sum_{l=0}^{\infty}\sum_{l'=0}^{\infty}\mathrm{Re}[C_l^+ C_{l'}^{+*} + 3C_l^- C_{l'}^{-*}]P_l(\cos\theta)P_{l'}(\cos\theta). \tag{18}$$

We write

$$C_l^{\pm} = \frac{4\pi i}{\sqrt{3k_i}}(A_l^{\pm} + iB_l^{\pm})$$

with

$$\begin{aligned} A_l^{\pm} &= (l+1)K^{\pm}(l, l+1)\cos\zeta_{l,l+1}^{\pm} - lK^{\pm}(l, l-1)\cos\zeta_{l,l-1}^{\pm} \\ B_l^{\pm} &= (l+1)K^{\pm}(l, l+1)\sin\zeta_{l,l+1}^{\pm} - lK^{\pm}(l, l-1)\sin\zeta_{l,l-1}^{\pm} \end{aligned} \tag{19}$$

and the appropriate modification for $l = 0$. Define (for $\mu = 0$)

$$A_{(0)}^{\pm} = \sum_{l=0}^{\infty} A_l^{\pm} P_l(\cos\theta), \qquad B_{(0)}^{\pm} = \sum_{l=0}^{\infty} B_l^{\pm} P_l(\cos\theta), \tag{20}$$

then, after some algebra, we obtain

$$\sigma_0(\theta) = \frac{k_f}{3k_i}[A_{(0)}^{+2} + B_{(0)}^{+2} + 3(A_{(0)}^{-2} + B_{(0)}^{-2})]. \tag{21}$$

The analysis for $\mu = 1$ is identical except that for this case we replace $A_{(0)}^{\pm}$, $B_{(0)}^{\pm}$ by

$$A_{(1)}^{\pm} = \sum_{l=1}^{\infty} \mathscr{A}_l^{\pm} P_l^1(\cos\theta), \qquad B_{(1)}^{\pm} = \sum_{l=1}^{\infty} \mathscr{B}_l^{\pm} P_l^1(\cos\theta) \tag{22}$$

with

$$\begin{aligned} \mathscr{A}_l^{\pm} &= \frac{1}{\sqrt{2}}(K^{\pm}(l, l+1)\cos\zeta_{l,l+1}^{\pm} + K^{\pm}(l, l-1)\cos\zeta_{l,l-1}^{\pm}) \\ \mathscr{B}_l^{\pm} &= \frac{1}{\sqrt{2}}(K^{\pm}(l, l+1)\sin\zeta_{l,l+1}^{\pm} + K^{\pm}(l, l-1)\sin\zeta_{l,l-1}^{\pm}) \end{aligned} \tag{23}$$

and $\sigma_0(\theta)$ by $\sigma_1(\theta)$.

It has been shown by Macek and Jaecks (1971) that information on the ratio of the $\mu = 0$ to the $\mu = 1$ differential cross section may be obtained from electron-photon

coincidence experiments. Such measurements provide a sensitive test of theoretical predictions. They have been carried out for the excitation of the 2^1P and 3^1P states of helium by Eminyan *et al* (1973, 1974). One quantity of interest is the dimensionless parameter

$$\lambda = \sigma_0/(\sigma_0+2\sigma_1) = \sigma_0/\sigma \tag{24}$$

and it is readily obtained in our models from (20)–(22) above.

The more delicate question of the measurement of the alignment and orientation parameters of the 2p state of atomic hydrogen, excited by electron impact (Fano and Macek 1973), and our theoretical predictions for these parameters will be discussed in IV (Morgan and McDowell 1975).

2.2. *Inclusion of coupling terms*

As in II, we can improve our model by retaining the full polarized orbital in the direct term of the transition matrix, consistent with neglecting exchange polarization in (I.11). Thus (1) above is replaced by

$$\tilde{T}_{\rm if}^{\pm} = T_{\rm if}^{\pm} + \langle \phi_{np\mu}(Z, 1)\chi_{\boldsymbol{k}_{\rm f}}(\boldsymbol{r}, 2)|V_{\rm f}|\phi_{\rm pol}(1, 2)F^{\pm}(2)\rangle \tag{25}$$

where $\phi_{\rm pol}(1, 2)$ is defined by (II.3) and (II.4). The subsequent analysis is straightforward and the result in this improved DWPO II model is to replace $I^{\pm}(l, l\pm1)$, equation (6) above, by

$$\tilde{I}^{\pm}(l, l\pm1) = I^{\pm}(l, l\pm1) + N^{\pm}(l, l\pm1) \tag{26}$$

with

$$N^{\pm}(l, l+1) = \int_0^{\infty} U_{l\pm1}^{\pm}(k_{\rm i}, r)H_l(k_{\rm f}, r)t_{1s,np}(r)\,{\rm d}r, \tag{27}$$

the kernel being given by

$$t_{1s,np}(r) = -\frac{4}{5r^4}\int_0^r U_{1s\rightarrow p}(s)R_{np}(s)s^3\,{\rm d}s \tag{28}$$

where $U_{1s\rightarrow p}(y)$ is the Sternheimer function defined in II. For the 2p case this kernel becomes

$$t_{1s,sp}(r) = -\frac{2}{5\sqrt{6Z}}\frac{1}{\alpha^3}\frac{1}{x^4}[2400-(\tfrac{1}{3}x^7+\tfrac{10}{3}x^6+20x^5+100x^4+400x^3+1200x^2 + 2400x+2400)\,{\rm e}^{-x}] \tag{29}$$

with $\alpha = \frac{3}{2}$ and $x = \alpha zr$. At small values of x,

$$t_{1s,2p}(r) \underset{x\rightarrow0}{\rightarrow} -\frac{16x^3}{35\times27\sqrt{6Z}}\left(1-\frac{7}{12}x+\frac{7}{54}x^2-\frac{7}{792}x^4\ldots\right). \tag{30}$$

3. Numerical methods

The evaluation of expressions for total and differential cross sections for dipole transitions is difficult because of the long-range nature of the interaction. The problem has

been extensively discussed, in the case of the CBO I approximation by Burgess *et al* (1970), and an elegant method for dealing with the necessary Coulomb integrals has recently been reviewed by Norcross (1973).

In our case the difficulties are confined to the $I^{\pm}(l, l\pm 1)$ integrals which may be written

$$I^{\pm}(l, l\pm 1) = \int_0^{\infty} U^{\pm}_{l\pm 1}(k_i, r) H_l(k_f, r) r f_{1s,np}(r)\, dr$$

and, for example

$$rf_{1s,2p}(r) = \frac{2^8}{3^4\sqrt{6}}\left[\frac{1}{x} - \left(\frac{1}{x} + \alpha + \frac{1}{2}\alpha^2 x + \frac{1}{8}\alpha^3 x^2\right) e^{-\alpha x}\right] \tag{31}$$

$$rf_{1s,3p}(r) = \frac{3^4}{2^6\sqrt{6}}\left[\frac{1}{x} - \left(\frac{1}{x} + \delta + \frac{1}{2}\delta^2 x + \frac{1}{12}\delta^3 x^2 - \frac{1}{24}\delta^4 x^3\right) e^{-\delta x}\right] \tag{32}$$

with $\delta = \frac{4}{3}$. Now

$$U^{\pm}_{l\pm 1}(k_i, r) \underset{r\to\infty}{\to} k^{-1/2} \sin[\phi(\alpha_0, k_i, r) + \delta^{\pm}_{l\pm 1}] \tag{33}$$

and

$$H_l(k_f, r) \underset{r\to\infty}{\to} \sin[\phi(0, k_f, r)]/k_f r \tag{34}$$

where $\phi(\alpha, k, r)$ is given by Burgess (1963) and depends on the polarizability α_0 of the target, while $\phi(0, k, r)$ is the normal Coulomb form. It follows that the integrand converges only as r^{-2} at large r.

We write

$$I^{\pm}(l, l\pm 1) = \int_0^a U^{\pm}_{l\pm 1}(k_i, r) H_l(k_f, r) r f_{1s,np}(r)\, dr + \int_a^b \tilde{U}^{\pm}_{l\pm 1}(k_i, r) H_l(k_f, r) r f_{1s,np}(r)\, dr$$
$$+ k_i^{-1/2} \int_b^{\infty} \sin[\phi(\alpha_0, k_i, r) + \delta^{\pm}_{l\pm 1}] H_l(k_f, r) \frac{a_n}{Zr}\, dr \tag{35}$$

in which $\tilde{U}^{\pm}_{l\pm 1}(k_i, r)$ is the WKBJ approximation to $U^{\pm}_{l\pm 1}(k_i, r)$. Typically we find suitable choices of a and b are of order $20a_0$ and $40a_0$ for $Z = 2$. The first two integrals in (35) are evaluated by Simpson's rule. The long-range contribution is evaluated by a variant of the method given by Belling (1968). For $l > l_0$ where l_0 is such that $|\delta^+_{l_0} - \delta^-_{l_0}| < 0{\cdot}01$ we neglect exchange in determining $U^{\pm}_l(k_i, r)$, while for $l > l_1$ (where l_1 is such that the non-exchange phaseshift $\delta_l < 0{\cdot}01$) we replace $U^{\pm}_l(k_i, r)$ by a Coulomb (or Bessel) function. Typical values of l_0 and l_1 at 100 eV are 8 and 11. At very large $l(l > 30)$ the J integrals become neglible and as a consequence of the centrifugal potential $l(l+1)/r^2$ the detailed nature of the I integrand is unimportant at small r. Thus if more than 30 partial waves are required for the convergence of equations (15) and (18), we omit the J integrals for $l \geqslant 30$ and replace rf_{1s2p} by its asymptotic form

$$r\tilde{f}_{1s,2p} = \left(\frac{2^8}{3^4 6^{1/2}}\right)\frac{1}{zr}$$

and evaluate the modified I integrals on $(0, \infty)$ analytically. Similar approximations may be made for $n \geqslant 3$. The details of the analysis will be reported elsewhere. Since we needed differential as well as total cross sections it was not found convenient to use the approximation (asymptotic in l) suggested by Burgess *et al* (1970) to correct the total cross section

$$Q_{1s\rightarrow np\mu} = \sum_{l=0}^{l_2} Q_l + \delta Q(l_2).$$

We agree with the expression for $\delta Q(l_2)$ given by those authors (their equation A42) but could not confirm their numerical results in the CBO I approximation, though our values for Q_l agreed with their tabulated values to four figures. The error involved is small over the range of energies for which they give results, but is significant at higher energies. A comparison is presented in table 1.

Table 1. $e + He^+(1s) \rightarrow e + He^+(2p)$. Total cross section in units of πa_0^2.

	CBO I approximation	
k_i^2 (Ryd)	Burgess *et al* (1970)	Our result
4	8·83, −2	8·83, −2
6	8·21, −2	8·20, −2
8	7·81, −2	7·79, −2
12	6·98, −2	6·94, −2
16	6·25, −2	6·20, −2

We find that to obtain convergence of the differential cross sections at large angles the number of partial wave contributions retained in the sums (20) and (22) above should be approximately equal to the excitation energy in electron volts. Thus at 200 eV at least 200 partial waves contribute at angles greater than 120°. Numerical difficulties arise, to some extent due to the use of a recursion relation for the Legendre functions $P_l^{\mu}(\cos\theta)$ for large l and large angle. It is then more convenient to replace in the DWPO I approximation $T^{\pm}_{1s\rightarrow 2p0}$ in (2) by

$$T^{\pm}_{1s\rightarrow 2p0} = \sum_{l=0}^{l_{max}} (C_l^{\pm} - d_l) P_l(\cos\theta) + F_{2p0} \tag{36}$$

where F_{2p0} is the Born approximation to the T matrix, and has the expansion

$$F_{2p0} = \sum_{l=0}^{\infty} d_l P_l(\cos\theta) \tag{37}$$

with $l_{max} = l_1$. A similar modification is made for $\mu = 1$.

4. Results and discussion

We report, in this paper, our results in both the DWPO I and DWPO II approximations for the total cross section for 1s → 2p excitation of H and of He^+ at energies up to 200 Z^2 eV.

In addition we give differential cross sections for

$$e + H(1s) \rightarrow e + H(2p)$$

at selected energies up to 50 eV. We also present our results for Ly α polarization at 90° to the incident beam ($P(90°)$) and values of the orientation parameter λ at selected energies.

Less detailed results on the 3p and 4p excitation cross sections are given, in the DWPO I approximation only, and in the case of atomic hydrogen total $n = 3$ cross sections are calculated and compared with experimental results.

4.1. Hydrogen: total cross section for np excitation

We shall show later by considering the 90° polarization of Ly α (§ 4.3) that we do not obtain reliable results in our models at energies below 1 Ryd. This is not unexpected, as we are in a single-channel representation, and no account is taken of the low-energy resonances. Our present results (table 2) are in poor agreement with those of more specialized calculations such as the close-coupling (Burke *et al* 1967a,b, Taylor and Burke 1967) or algebraic variational method (Callaway and Wooten 1974, 1975) in the energy range from threshold to 0·95 Ryd. Furthermore, in this range those specialized calculations are in close agreement with recent absolute measurements (Long *et al* 1968, Williams and Willis 1974). However, even close to threshold both our models give an order of magnitude improvement over the Born–Oppenheimer approximation (table 2). Nevertheless we must conclude that the excellent agreement with the close-coupling and algebraic variation method results obtained in II for the 1s → 2s transition at energies below 0·85 Ryd must be regarded as a coincidence.

We believe our results are significant above the ionization threshold, where resonance structure no longer dominates. The two models give substantially different results. The

Table 2. Calculated cross sections for the process $e + H(1s) \rightarrow e + H(2p)$ (in units of πa_0^2): Q_1 (DWPO I), Q_2 (DWPO II) this paper, Q_{BO} (Born–Oppenheimer), Q_B (Born), Q_{CPB} (Coulomb-projected Born, Geltman and Hidalgo 1971), Q_{BCS} (four-state impact parameter, Bransden *et al* 1972), Q_{CC} (a, three-state close coupling with correlation, Taylor and Burke 1967; b, algebraic variational method, Callaway and Wooten 1974, 1975).

k^2 (Ryd)	0·76	0·78	0·8	0·85	0·90	1·0	1·5	2·0	3·0
Q_1	0·0860	0·144	0·185	0·276	0·365	0·536	0·987	1·094	1·075
Q_2	0·076	0·126	0·161	0·237	0·312	0·455	0·820	0·912	0·913
Q_{BO}	1·082	1·650	1·885	2·013	1·924	1·661	1·190	1·14	1·065
Q_{CC}	0·2387a	0·2332a	—	0·3509a	0·369b	0·493b	—	—	—
k^2 (Ryd)	3·675	4·0	5·0	6·0	7·0	7·35	11·025	14·7	
E (eV)	50·0	54·4	68·0	81·6	95·2	100	150	200	
Q_1	1·020	0·991	0·905	0·829	0·763	0·743	0·581	0·481	
Q_2	0·875	0·854	0·788	0·728	0·675	0·658	0·522	0·435	
Q_{BO}	1·002	0·972	0·886	0·812	0·799	0·729	0·573	0·475	
Q_B	—	—	—	—	—	0·750	—	0·480	
Q_{CPB}	—	—	—	—	—	0·821	—	0·509	
Q_{BCS}	—	—	—	—	—	0·736	—	0·475	

simpler DWPO I model gives total 2p cross sections lying slightly above those obtained by Sullivan *et al* (1972) in their four-state impact-parameter version of the second-order optical potential method (Bransden *et al* 1972), and approaches the Born approximation from below at 100 eV, lies above Born to 200 eV, and at higher energies is in close agreement with Born (figure 1).

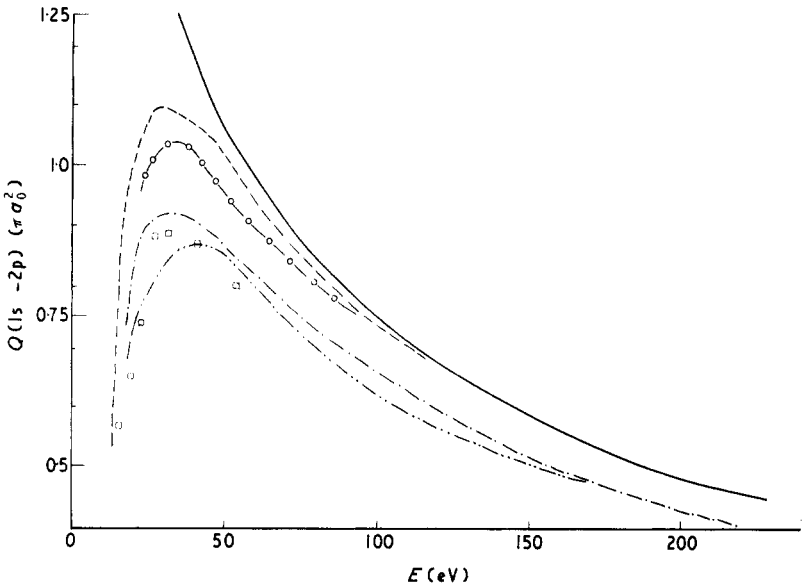

Figure 1. Theoretical predictions for the total cross section for e + H(1s) → e + H(2p). Full curve, Born; – – –, DWPO I and – · – · –, DWPO II (this paper); –o–o–, Sullivan *et al* (1972) four-state; – – · · · – – · ·, Flannery and McCann (1974) three-state; □, pseudo-states (Burke and Webb 1972).

The DWPO II results, which take account of s–p coupling, are significantly lower at all energies. The general behaviour shown is similar to that obtained by Flannery and McCann (1974) in their three-state eikonal model, the differences being less than 10%. This model is an approximation to the three-state close-coupling model, but retains all partial waves. At low energies ($13{\cdot}6 < E < 40$ eV) our results also agree well with the pseudo-state calculation of Burke and Webb (1970).

Our results in the DWPO II approximation are compared with the experiment of Long *et al* (1968) at energies $20 \leqslant E \leqslant 200$ eV in figure 2. The energy dependence of the theoretical result is not the same as that of the experiment. If the experiment is renormalized downward by 10% to bring it into accord with our theory at 200 eV, the resulting maximum cross section of $0{\cdot}77\ \pi a_0^2$ at 40 eV is in worse accord with the theoretical maximum of $0{\cdot}91\ \pi a_0^2$ at that energy. Alternatively if the experiment is renormalized to the absolute value of $0{\cdot}276^{+0{\cdot}026}_{-0{\cdot}016}\ \pi a_0^2$ at 11·02 eV measured by Williams and Willis (1974), while the maximum of $0{\cdot}92\ \pi a_0^2$ is then in close accord with the result of our calculation, the consequent experimental value of $0{\cdot}52\ \pi a_0^2$ at 200 eV is now 15% above the calculated value. Perhaps the most satisfactory adjustment is to accept the Long *et al* data as correct: theory and experiment are then in agreement to 10% or better at all energies $20 \leqslant E \leqslant 200$ eV.

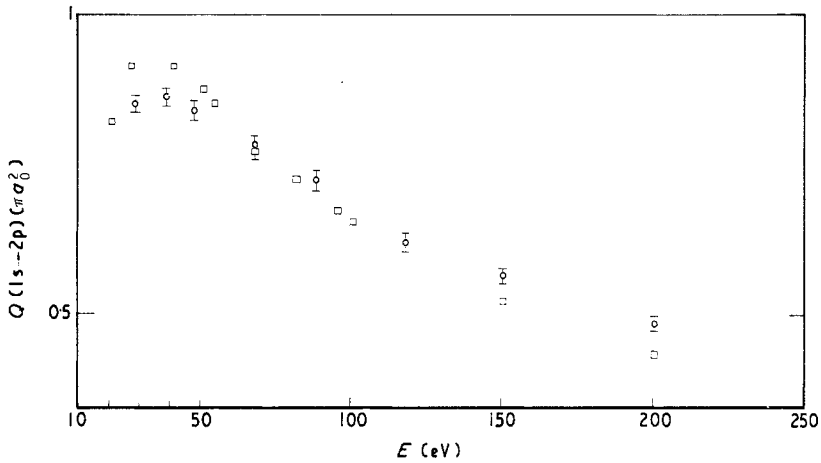

Figure 2. Total cross section for e + H(1s) → e + H(2p). The ○ are the measurements of Long *et al* (1968), the □ the DWPO II theoretical values.

Cascade effects are small for this transition. Long *et al* estimate them as 2% at 200 eV. The cascade correction may be approximated by (Morrison and Rudge 1966)

$$Q_{\text{cas}}(1s \rightarrow 2p) = Q(1s, 3s) + Q(1s, 3d) + 0{\cdot}58Q(1s, 4s) + 0{\cdot}04Q(1s, 4p). \quad (38)$$

We have calculated $Q(1s, 4p)$ in the DWPO I model at 100 and 200 eV (see table 3(*a*)), while the results for the $1s \rightarrow ns$ transitions are given in I. Adopting Morrison and Rudge's Born values for $Q(1s \rightarrow 3d)$ we find that $Q_{\text{cas}}(1s \rightarrow 2p)$ is less than the assigned experimental error in the $1s \rightarrow 2p$ cross section at energies above 100 eV.

Our results for the total $1s \rightarrow 3p$ and $1s \rightarrow 4p$ cross sections in the DWPO I model are compared with the Born–Oppenheimer results in table 3(*a*). It is clear that distortion effects of the DWPO I type considered here are insignificant with respect to total cross sections at energies above 40 eV.

On the assumption that the Born approximation results for the $1s \rightarrow 3d$ transition are adequate above 30 eV we can combine these with the present DWPO I results to obtain total $n = 3$ (table 3(*b*)).

Experimental measurements of the total $n = 3$ excitation cross section have been reported by Kleinpoppen and Kraiss (1968) and more recently by Mahan *et al* (1975). More precisely, they measure the Balmer α line excitation function and normalize to the Born approximation above 300 eV (Kleinpoppen and Kraiss) or at 500 eV (Mahan *et al*). The equivalent cross section is

$$Q(\text{H}\alpha) = Q_{3s} + 0{\cdot}12Q_{3p} + Q_{3d}. \quad (39)$$

We use our DWPO I results for the 3s and 3p cross sections, together with Born values for 3d to obtain the theoretical results given in table 3(*c*), where we compare them with the experimental results. This comparison is shown also, together with the Born approximation results, in figure 3, and suggests that the more recent experimental results are to be preferred. However more detailed comparison with the data of Mahan (1974) indicates that the observed 3d cross section is much larger than the Born values we adopt, while the experimental values for $0{\cdot}12Q_{3p}$ are substantially smaller than our DWPO I values. We are therefore evaluating the separate $n = 3$ cross sections in the DWPO II model in order to elucidate these points (Syms *et al* 1975).

Table 3. (a) Cross sections for the processes e+H(1s) → e+H(*n*p), $n = 3, 4$ in DWPO I and Born–Oppenheimer approximations in units of πa_0^2.

	E (eV)	20	30	40	50	100	150	200
$n = 3$	Q_1	0·148	0·180	0·178	0·170	0·126	0·098	0·081
	Q_{BO}	0·228	0·189	0·178	0·168	0·123	0·096	0·080
$n = 4$	Q_1	—	—	—	—	0·044	—	0·029
	Q_{BO}	—	—	—	—	0·043	—	0·028

(b) Total $n = 3$ cross sections (πa_0^2), see text.

E (eV)	Q_1 (3s)	Q_1 (3p)	Q_{BORN} (3d)	Total
20	0·015	0·148	(0·022)	0·19
30	0·018	0·180	0·021	0·22
40	0·017	0·178	0·019	0·21
50	0·015	0·170	0·017	0·20
100	0·009	0·126	0·009	0·145
150	0·007	0·098	0·007	0·11
200	0·005	0·081	0·005	0·09

(c) Theoretical and experimental cross sections for Balmer α production (πa_0^2).†

E (eV)	Theory (this paper)	Mahan (1974)	Kleinpoppen and Kraiss (1968)
20	0·055	0·067	0·036
30	0·061	0·059	0·036
50	0·051	0·051	0·037
80	0·039	0·036	0·035
200	0·020	0·019	0·019
500	0·010	0·010	0·010

RMS errors on the measurements are indicated in figure 3.

The Glauber results of Tai *et al* (1970) (as amended by Mahan (1974) to include the 3d Born contribution) are also shown in figure 3. Both our results and the Glauber results are consistent with the experiment of Mahan *et al* at 50 eV and above, though DWPO I remains in accord down to 30 eV whereas Glauber fails below 50 eV.

4.2. Hydrogen: differential cross sections

There are no experimental measurements of the 1s → 2p differential cross section at low energies. A detailed comparison of our results with other theoretical models and with intermediate energy ($50 \leqslant E \leqslant 200$ eV) experiments given in V (McDowell *et al* 1975).

We do not expect our model to be reliable below the ionization threshold, so in table 4 we give differential cross sections at 1·0, 1·5, 2·0 and 3·0 Ryd for the 1s → 2p transition only.

† *Note added in proof.* Smith (1975 private communication) suggests that the experimental results are a few per cent higher at low energies. See Syms *et al* (paper VI of this series) for a full discussion.

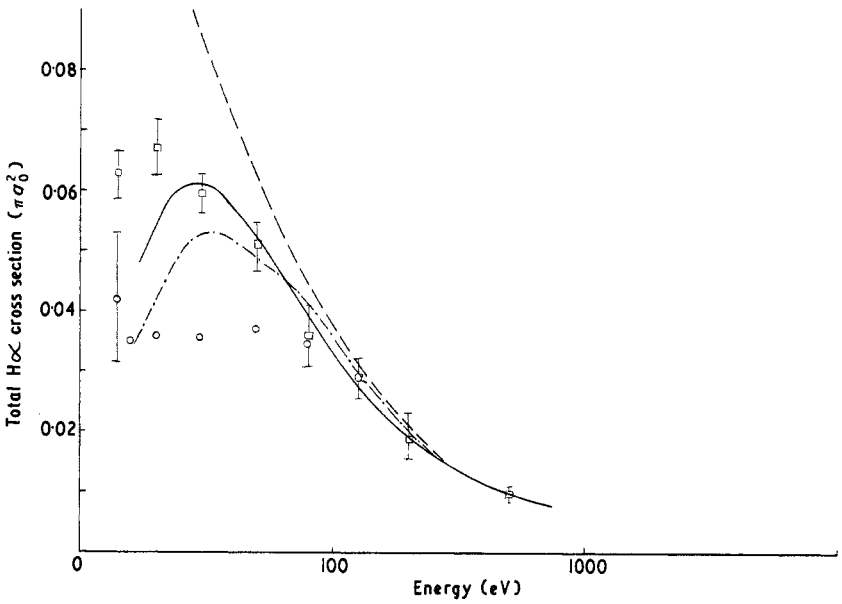

Figure 3. Cross section for the Hα production in units of πa_0^2. The experimental values of Mahan (1974) are shown by ⊡ and those of Kleinpoppen and Kraiss (1968) by ⊙. The full curve is the modified DWPO I approximation of this paper (see text), the broken curve is the Born approximation, and the chain curve the Glauber approximation (Tai *et al* 1970, Bhadra and Ghosh 1971).

Close-coupling (CC) calculations have been reported by Scott (1965), using 1s–2s–2p R-matrix elements of Burke *et al* (1963), and more recently by Brandt and Truhlar (1974). These authors criticize Scott's work, and compare three-state and six-state close coupling results. Their results are compared with the DWPO II predictions, for an energy $k^2 = 1$ Ryd, in figure 4. Both approximations are in close agreement except for angles

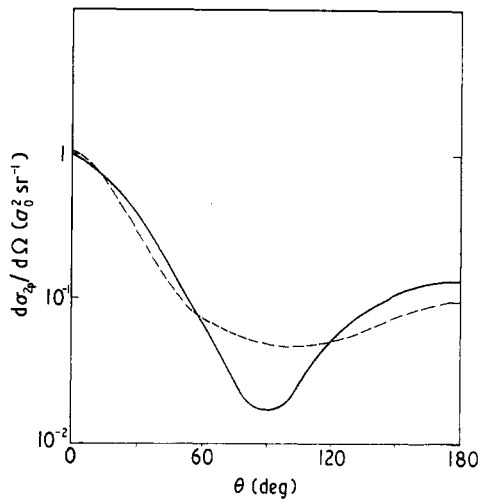

Figure 4. Differential cross sections for e + H(1s) → e + H(2p) at $k^2 = 1{\cdot}0$ (13·6 eV). Full curve DWPO II, this paper; broken curve six-state close coupling (Brandt and Truhlar 1974).

$60° < \theta < 120°$ where the six-state CC results do not show the deep minimum obtained in our model.

The 2p excitation cross section measured by Williams and Willis (1974) at energies below 0·85 Ryd are in excellent agreement with the three-state CC plus correlation calculations of Taylor and Burke (1967). However the corresponding six-state results (Burke *et al* 1967a, b) lie 25% higher at $k^2 = 0{\cdot}85$. It is therefore unclear how reliable the differential cross sections obtained from Burke's R-matrix elements by Brandt and Truhlar (1974) are. Furthermore Brandt and Truhlar comment that their results at $k^2 = 1$ may not have converged with respect to summation over partial waves.

As the energy increases from $k^2 = 1{\cdot}0$ to $k^2 = 3{\cdot}0$ the forward peak is enhanced, and the back scattering becomes less important, though there is always a shallow minimum which moves out to larger angles as the energy increases.

Table 4. Differential cross sections for e + H(1s) → e + H(2p) (in the DWPO II model, units of $a_0^2\,\mathrm{sr}^{-1}$).

θ (deg)	k^2 (Ryd)			
	1·0	1·5	2·0	3·0
0	9·77, −1	5·83, 0	1·26, 1	2·77, 1
15	7·55, −1	2·83, 0	3·73, 0	3·39, 0
30	3·95, −1	7·23, −1	5·63, −1	2·64, −1
45	1·74, −1	2·13, −1	1·20, −1	3·61, −2
60	7·17, −2	8·77, −2	4·12, −2	1·05, −2
90	1·68, −2	1·22, −2	5·71, −3	1·76, −3
120	5·32, −2	1·36, −2	4·49, −3	1·08, −3
150	1·11, −1	3.20, −2	8·92, −3	1·44, −3
180	1·36, −1	3·79, −2	1·09, −2	1·66, −3

Results in both models (DWPO I, DWPO II) for small angle $n = 2$ differential scattering at 50 eV are compared in figure 5 with the absolute experimental measurements of Bohm (1974) (a calibration of the earlier relative measurement by Williams (1969)), and Williams and Willis (1975), both taken at 54·4 eV. The agreement is excellent over the restricted range of angles for which experimental data is available; however as will be seen in V, at large angles our models retain only qualitative validity. Furthermore, in this angular range ($\theta \leqslant 30°$) our results are essentially identical at 50 eV to the Glauber results of Gosh *et al* (1970), though both are in much better agreement with experiment than the Born or four-state impact-parameter second-order potential method (Sullivan *et al* 1972).

4.3. Polarization of Ly α radiation

The optical polarization of the Ly α radiation emitted at 90° to the incident electron beam following excitation of the 2p state has been measured by Ott *et al* (1970). The general theory has been given by Percival and Seaton (1958), the 90° result taking the simple form (Burke and Taylor 1967)

$$P(90°) = \frac{3(1-x)}{7+11x}, \qquad x = Q_1/Q_0. \tag{40}$$

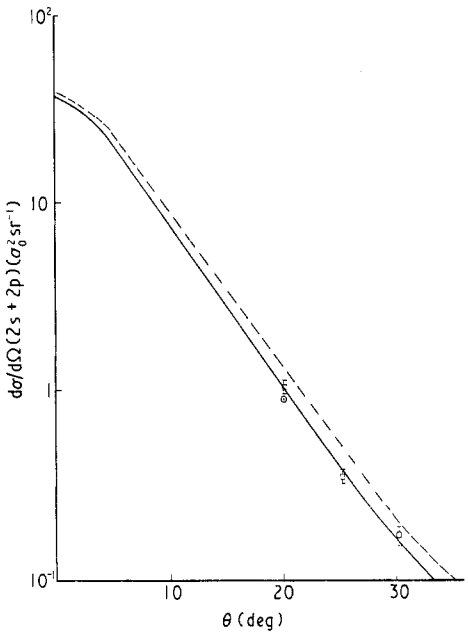

Figure 5. Differential cross section for $e + H(n = 1) \rightarrow e + H(n = 2)$ at 50 eV. Broken curve DWPO I, full curve DWPO II. The experimental points of Williams and Willis (1975) are shown as ⊟, and the calibration point of Bohm (1974) as a ⊙.

We tabulate our results in both models together with the experimental values, in table 5. The agreement is excellent, the DWPO II results being clearly superior at all energies above 20 eV. A graphical comparison with experiment and with the Born and Glauber predictions (Gerjuoy and Thomas 1974) is presented in figure 6.

Table 5. $P(90°)$ for $e + H(1s) \rightarrow e + H(2p)$.

E (eV)	DWPO I	DWPO II	Experiment
13·6	0·311	0·311	$0·24 \pm 0·02$
20·4	0·245	0·249	$0·22 \pm 0·02$
40·8	0·147	0·153	$0·16 \pm 0·02$
50·0	0·127	0·129	$0·13 \pm 0·01$
81·6	0·069	0·077	$0·075 \pm 0·01$
100·0	0·049	0·058	$0·050 \pm 0·005$
150·0	0·0126	0·0223	$0·020 \pm 0·01$
200·0	−0·010	0·0001	$0·0 \pm 0·01$

The experimental results are those of Ott *et al* (1970).

Clearly, our DWPO II results are in markedly better agreement with experiment for $E_i \geqslant 20$ eV than either Born or Glauber, but in common with these models our results are in poor accord with experiment below 20 eV, tending to the Percival and Seaton (1958) threshold value of 43 %. The measurements, however, tend to a value near 24 % close to threshold, which is well reproduced by close-coupling calculations (Taylor and Burke 1967), allowing for the beam energy distribution.

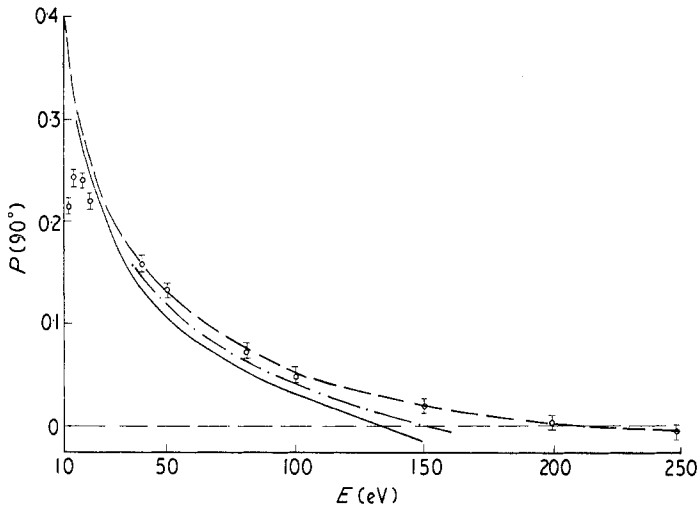

Figure 6. Polarization of Ly α at 90°. The experimental point of Ott *et al* (1972) are shown $\bar{\bigcirc}$, the theoretical curves being DWPO II (broken curve), Glauber (Gerjuoy and Thomas 1974) (chain curve) and Born (full curve).

4.4. The orientation parameter

The behaviour of the orientation parameter λ at low energies (k^2 = 1·0, 1·5 and 2·0) is illustrated in figure 7. Initially quite smooth with a single minimum near 90°, but with appreciable asymmetry, it rapidly develops structure as the energy increases. By k^2 = 1·5 Ryd the characteristic behaviour of λ in our DWPO II model is established: a rapid decrease from a value of 1·0 in the forward direction to a deep minimum near θ = 30°, a maximum near 90° followed by a second shallow minimum near 120°, returning to its initial value in the backward direction.

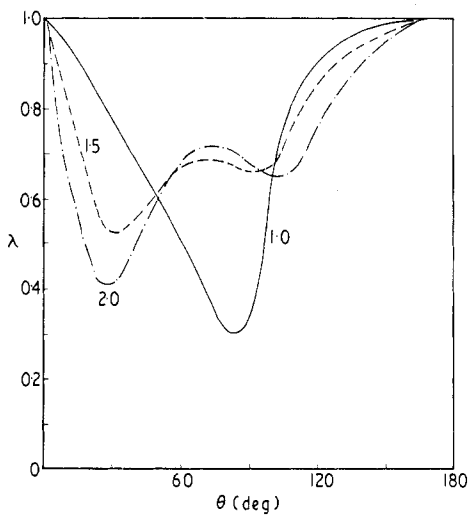

Figure 7. The orientation parameter $\lambda = \sigma_0/\sigma$ calculated in the DWPO II model at k^2 = 1, 1·5 and 2·0 Ryd.

The behaviour of λ at higher energies (50,100 and 200 eV) is shown in figure 8. The minima become deeper with increasing impact energies and move to smaller angles. The intermediate maximum also moves to smaller angles and by 200 eV is at 30°.

Our present DWPO II results are compared with the Born approximation in figure 9. The first Born (and related approximations) forbids transfer of angular momentum along $\boldsymbol{K} = \boldsymbol{k}_i - \boldsymbol{k}_f$. Consequently in our reference frame (with Z axis along $\hat{\boldsymbol{k}}_i$) it gives

$$\lambda_B = \cos^2\theta_{\boldsymbol{K}} = \frac{(1 - x\cos\theta)^2}{1 + x^2 - 2x\cos\theta}, \qquad x = k_f/k_i. \tag{41}$$

The comparison with the DWPO II results shows that at 100 eV the Born approximation fails for scattering angles $\theta > 10°$, neither the maximum near 45° nor the second minimum occurring. Nevertheless except for the forward direction ($\theta = 0$) the first Born approximation gives an accurate account of the total differential cross section out to about $\theta = 35°$. We suggest that measurements of λ are a more sensitive indication of

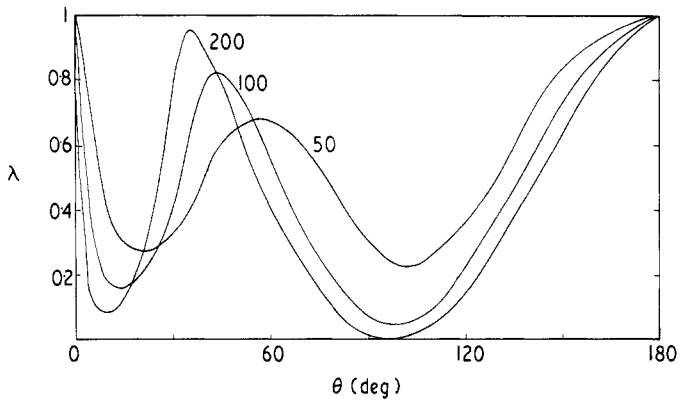

Figure 8. As for figure 7 but at 50, 100 and 200 eV.

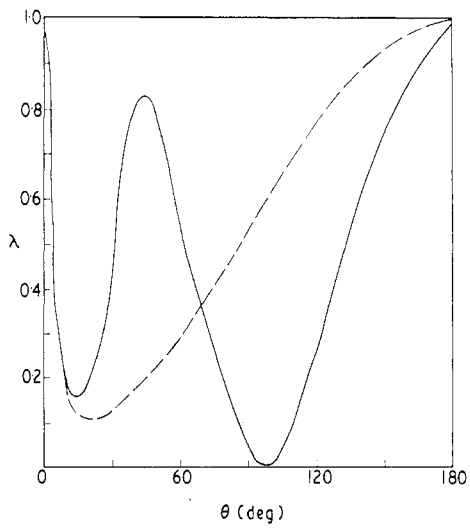

Figure 9. The DWPO II values of λ (full curve) and the Born result (broken curve) at 100 eV.

departures from first Born behaviour than are measurements of the differential cross section.

4.5. He^+: total and differential cross sections

Our total cross sections for $e + He^+(1s) \rightarrow e + He^+(2p)$ are given in table 6(*a*) and are compared with the CBO I approximation in figure 10 at energies up to 90 eV. Again, resonance effects below the inelastic threshold are not included in our models, so that our results are unlikely to be accurate at energies below 50 eV for He^+.

Table 6. (a) Total cross sections (in units of πa_0^2) for $e + He^+(1s) \rightarrow e + He^+(np)$, $n = 2$ in the DWPO I approximation, and in the DWPO II approximation.

k_i^2 (Ryd)	3·005	3·2	3·6	4·0	4·5	5·0	6·0
$Q_{1s\rightarrow 2p}$ (I)	7·47, −2	7·77, −2	8·09, −2	8·21, −2	8·26, −2	8·26, −2	8·18, −2
$Q_{1s\rightarrow 2p}$ (II)	7·15, −2	7·25, −2	7·48, −2	7·55, −2	7·56, −2	7·54, −2	7·46, −2
k_i^2 (Ryd)	8·0	12·0	14·0	16·0	20·0	25·0	30·0
$Q_{1s\rightarrow 2p}$ (I)	—	7·06, −2	—	6·26, −2	5·70, −2	5·07	4·57, −2
$Q_{1s\rightarrow 2p}$ (II)	7·2, −2	6·54, −2	6·21, −2	5·89, −2	5·32, −2	4·76, −2	4·31, −2

(b) Total cross sections for $e + He^+(1s) \rightarrow e + He^+(3p)$ in the DWPO I approximation (units of $10^{-2}\pi a_0^2$).

k^2 (Ryd)	3·6	4·0	4·5	5·0	6·0	8·0
$Q_{1s\rightarrow 3p}$	1·38	1·45	1·46	1·44	1·40	1·33
k^2 (Ryd)	12·0	14·0	16·0	20·0	25·0	30·0
$Q_{1s\rightarrow 3p}$	1·19	1·13	1·07	0·96	0·96	0·77

Our threshold values are $7{\cdot}44 \times 10^{-2}\ \pi a_0^2$ in the DWPO I model and $7{\cdot}15 \times 10^{-2}\ \pi a_0^2$ in the DWPO II, whereas Burgess *et al* (1970) obtain $10{\cdot}08 \times 10^{-2}\ \pi a_0^2$ in the CBO I model. Burke and Taylor (1969) have used a 1s–2s–2p close-coupling expansion with twenty correlation terms, at energies below the $n = 3$ threshold. Their threshold value of $4{\cdot}88 \times 10^{-2}\ \pi a_0^2$ is much lower than ours, whereas (II), their result for 1s → 2s was almost a factor of three higher. It will be noticed that Burke and Taylor (1969) find a strong ^1P resonance in the 1s → 2p excitation cross section near $k^2 = 3{\cdot}34$ Ryd (figure 10), that is, just below the $n = 3$ threshold. We would expect their calculation to be much more reliable than ours at this energy. Our model should have considerable validity for $k^2 \geqslant 4{\cdot}0$ Ryd ($E_i \geqslant 54{\cdot}4$ eV), and (figure 10) gives substantially lower values than the CBO I approximation at energies up to 80 eV in both models. The smaller target polarizability and the enhanced role of the Coulomb interaction ensures that the departure from the CBO I approximation in DWPO I are comparatively small compared with those found with the Born and Born–Oppenheimer approximations in the neutral case.

The classically scaled Born value for $He^+(1s \rightarrow 2p)$ at 400 eV is $4{\cdot}69 \times 10^{-2}\ \pi a_0^2$, whereas we obtain $4{\cdot}31 \times 10^{-2}\ \pi a_0^2$ in the DWPO II model, a reduction of almost 9%. If classical scaling fails to this extent for higher 1s → *n*p transitions, then the estimate of the

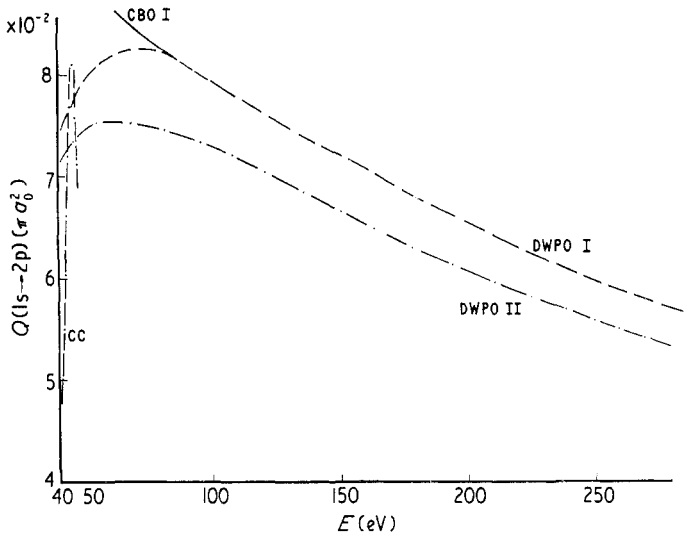

Figure 10. Total cross section for $e + He^+(1s) \rightarrow e + He^+(2p)$, in units of πa_0^2. The full curve shows the CBO I result (Burgess *et al* 1970), the DWPO I and DWPO II curves being labelled. The sharply peaked curve at low energies represents the close-coupling calculation of Burke and Taylor (1967).

cascade contribution to the observed 1s → 2s cross section (Dolder and Peart 1973) of $0{\cdot}23\sigma(3p)$ adopted in I is 10 % too large. The effect would be to increase the experimental values by about half this amount (5 %) at threshold, bringing them slightly closer to the Burke and Taylor (1969) result, and slightly increasing the discrepancy with our DWPO II values (of II). Detailed DWPO II calculations on the 1s → 3p transition are in progress (Syms *et al* 1975). Results for this transition have been obtained in the DWPO I model, and values of the total cross section at selected energies are presented in table 6(*b*).

We have also calculated the differential cross section ($d\sigma/d\Omega$), $P(90°)$, λ and the Fano–Macek parameters and values for these quantities may be obtained from the authors, at all the above energies for 2p and 3p and for 4p at selected energies.

5. Conclusions

We have applied the distorted wave polarized orbital models of I and II to 1s → *n*p ($n = 2, 3, 4$) transitions in H and He^+ over a wide range of energies (from threshold to $20Z^2$ Ryd) with encouraging success.

It is clear that such models do not give accurate predictions at energies below the ionization threshold, but at higher energies, give an accurate account of the observable phenomena, where these have been measured, and are in reasonable accord with other sophisticated theoretical models at moderate and high energies.

In particular the DWPO II results agree well with six-state close-coupling calculations of differential cross sections for 1s → 2p in atomic hydrogen at energies as low as 1 Ryd for all angles outside the range $60 < \theta < 120°$. The predicted values for the 90° polarization of Ly α are in excellent agreement with the experimental results of Ott *et al* (1970) at all energies above 20 eV.

Total 1s → 2p cross sections for electron excitation of atomic hydrogen agree well (within 10%) with the absolute measurements of Williams and Willis (1974) and of Long *et al* (1968) at energies from 20 to 200 eV.

At intermediate energies the DWPO II 1s → (2p + 2s) differential cross sections are in excellent agreement with the absolute measurements of Bohm (1974) and of Williams and Willis (1975) at angles to 60°.

Again, calculated total Balmer α production cross sections (DWPO I) agree well with recent measurements by Mahan *et al* (1975) though some discrepancies remain.

We conclude that the DWPO II model is a reliable predictor for 1s → *n*p transitions in atomic hydrogen at energies above the ionization threshold, though its reliability decreases at angles $\theta > 60°$ for differential measurements.

Our results confirm that the first Born approximation is unreliable for total and differential cross sections at energies below 500 eV, and is never useful for large angle differential scattering. This conclusion is reinforced by the calculated values of the orientation parameter λ of the 2p state, which shows significant departures from the Born values for all angles ($\theta > 10°$) and energies treated here.

Similar calculations for *n*p excitations in He^+ suggest that classical scaling ($Z^4Q(Z^2k_i^2) =$ constant) fails by at least 10% for $Z^2k_i^2 \leqslant 20$, and may imply a significant change in the cascade corrections to measurements of the 1s → 2s cross section (of about −10%).

References

Belling J A 1968 *J. Phys.* B: *Atom. Molec. Phys.* **2** 136
Bhadra K and Gosh A S 1971 *Phys. Rev. Lett.* **26** 737–9
Bohm K 1974 private communication to J F Williams
Brandt M A and Truhlar D G 1974 *Phys. Rev.* A **9** 1188–94
Bransden B H, Coleman J P and Sullivan J 1972 *J. Phys.* B: *Atom. Molec. Phys.* **5** 537–45
Burgess A 1963 *Proc. Phys. Soc.* **81** 442–52
Burgess A, Hummer D G and Tully S A 1970 *Phil. Trans. R. Soc.* A **266** 255–79
Burke P G, Ormonde S and Whitaker W 1967a *Proc. Phys. Soc.* **92** 319–35
Burke P G, Schey H M and Smith K 1963 *Phys. Rev.* **129** 1258–74
Burke P G and Taylor J A 1969 *J. Phys.* B: *Atom. Molec. Phys.* **2** 44–51
Burke P G, Taylor J A and Ormonde S 1967b *Proc. Phys. Soc.* **92** 345–50
Burke P G and Webb T G 1970 *J. Phys.* B: *Atom. Molec. Phys.* **3** L131–3
Byron F W and Joachain C J 1973 *Phys. Rev.* A **8** 1267–82
Callaway J and Wooten J W 1974a *Phys. Rev.* A **9** 1924–31
—— 1975 *Phys. Rev.* A **4** in press
Dolder K T and Peart B 1973 *J. Phys.* B: *Atom. Molec. Phys.* **6** 2415–26
Eminyan M, McAdam K B, Slevin J and Kleinpoppen H 1973 *Phys. Rev. Lett.* **31** 576–9
—— 1974 *J. Phys.* B: *Atom. Molec. Phys.* **7** 1519–42
Fano U and Macek J H 1973 *Rev. Mod. Phys.* **45** 553–73
Flannery M R and McCann K J 1974 *J. Phys.* B: *Atom. Molec. Phys.* **7** L223–7
Geltman S and Hidalgo M B 1971 *J. Phys.* B: *Atom. Molec. Phys.* **4** 1299–307
Gerjuoy E and Thomas B K 1974 *Rep. Prog. Phys.* **37** 1345–431
Gosh A S, Sinha P and Sil N C 1970 *J. Phys.* B: *Atom. Molec. Phys.* **3** L58
Kleinpoppen H and Kraiss L 1968 *Phys. Rev. Lett.* **20** 361–3
Lloyd M D and McDowell M R C 1969 *J. Phys.* B: *Atom. Molec. Phys.* **2** 1313–22
Long R L, Cox D M and Smith S J 1968 *J. Res. Nat. Bur. Stand.* A **72** 521–35
Macek J and Jaecks D H 1971 *Phys. Rev.* A **4** 2288–300
McDowell M R C 1975 *Electron and Photon Interactions with Atoms* ed H Kleinpoppen and M R C McDowell (New York: Plenum Press) in press
McDowell M R C, Morgan L A and Myerscough V P 1973 *J. Phys.* B: *Atom. Molec. Phys.* **6** 1435–51

McDowell M R C, Morgan L A and Myerscough V P 1975 *J. Phys.* B: *Atom. Molec. Phys.* **8** to be published
McDowell M R C, Myerscough V P and Narain U 1974 *J. Phys.* B: *Atom. Molec. Phys.* **7** L195–7
McGowan J W, Williams J F and Curley E K 1969 *Phys. Rev.* **180** 132–8
Mahan H 1974 *PhD Thesis* University of Colorado
Mahan H, Gallaher A and Smith S 1975 *Phys. Rev.* to be submitted
Morgan L A and McDowell M R C 1975 *J. Phys.* B: *Atom. Molec. Phys.* **8** 1073–81
Morrison D J T and Rudge M H R 1966 *Proc. Phys. Soc.* **89** 45–53
Norcross D W 1973 *Comp. Phys. Commun.* **6** 257–64
Ott W R, Kaippila W and Fite W L 1970 *Phys. Rev.* A **1** 1089–98
Percival I C and Seaton M J 1958 *Phil. Trans. R. Soc.* **251** 113–38
Scott B L 1965 *Phys. Rev.* **140** A699–704
Sullivan J, Coleman J P and Bransden B H 1972 *J. Phys.* B: *Atom. Molec. Phys.* **5** 2061–5
Syms R, McDowell M R C, Morgan L A and Myerscough V P 1975 *J. Phys.* B: *Atom. Molec. Phys.* to be submitted
Taylor J A and Burke P G 1967 *Proc. Phys. Soc.* **92** 336–44
Tai H, Bassel R H, Gerjuoy E and Franco V 1970 *Phys. Rev.* A **1** 1819–35
Williams J F and Willis B A 1974 *J. Phys.* B: *Atom. Molec. Phys.* **7** L61–5
—— 1975 *J. Phys.* B: *Atom. Molec. Phys.* **8** to be published
Williams K G 1969 *Proc. 6th Int. Conf. on Physics of Electronic and Atomic Collisions* Abstracts (Cambridge, Mass: MIT) pp 731–4